Earth Return Path Impedances of Underground Cables for the Two-Layer Earth Case

Dimitrios A. Tsiamitros, Grigoris K. Papagiannis, *Member, IEEE*, Dimitris P. Labridis, *Senior Member, IEEE*, and Petros S. Dokopoulos, *Member, IEEE*

***Abstract*—The influence of earth stratification on underground power cable impedances is investigated in this paper. A rigorous solution of the electromagnetic field for the case of underground conductors and a two-layer earth is presented. Analytic expressions for the self and mutual impedances of the cable are derived. The involved semi-infinite integrals are calculated by a novel, numerically stable, and efficient integration scheme. Typical single-core cable arrangements are examined for a combination of layer depths and earth resistivities, based on actual measurements. The accuracy of the results over a wide frequency range is justified by a proper finite-element method formulation. The differences in cable impedances due to earth stratification are presented. Finally, a simple switching transient simulation is examined to evaluate the influence of the earth stratification on transient voltages and currents.**

***Index Terms*—Electromagnetic transient analysis, finite-element method (FEM), nonhomogeneous earth, power cable modeling.**

I. Introduction

In TRANSIENT simulations, detailed transmission-line modeling is required. In the case of underground power cables, the model parameters are strongly influenced by the resistive earth return path. The influence of the lossy earth on conductor impedances has been analyzed since 1926. For the case of overhead lines, proper earth correction terms can be calculated using the widely accepted Carson's formulas [1]. Similar formulas have been developed by Pollaczek [2], applicable not only to overhead conductor systems but also to cases of underground power cables and to combinations of both. In all of these approaches, the earth is assumed to be semi-infinite and homogeneous.

In practice, however, the earth is composed of several layers of different electromagnetic (EM) properties. Sunde [3] extended the homogeneous earth solution and proposed formulas for the case of a two-layer earth, but only for overhead lines or cables above or on the surface of the earth. In 1973, Nakagawa [4], [5] proposed a general solution for the case of overhead conductors above a multilayered earth model. However there is still lack of an analytic formulation for the case of underground conductors and multilayered earth structures.

The scope of this paper is to present new analytic formulas which can be used for the direct calculation of the self and mutual impedances of power cables buried in a two-layer earth. The expressions are derived by a rigorous and general solution of the EM field equations, using a methodology based on Sunde's approach [3]. Their form is similar to the corresponding expressions proposed by Pollaczek [2] and Sunde [3], containing semi-infinite integral terms. These terms are evaluated using a novel numerical integration scheme, based on proper combinations of numerical integration methods to overcome efficiently the problems due to the highly oscillatory form of the infinite integrals [6].

The accuracy of the results obtained by the new expressions is verified using a proper finite-element-method (FEM) formulation [7]. The impedances of typical single-core (SC) cable arrangements are calculated for various cases of two-layer earth models based on actual ground resistivity measurements [8].

The differences between the cable impedances calculated by the new formulas and those resulting by the well-known Electromagnetic Transients Program (EMTP) [9] for the case of homogeneous earth are also presented. Finally, the new formulas are used to calculate the impedances for a typical switching transient simulation, in order to evaluate the influence of the earth stratification on the actual transient voltages and currents. The resulting differences show that earth stratification must be taken into account especially in cases of unbalanced faults, where the earth return path plays an important role.

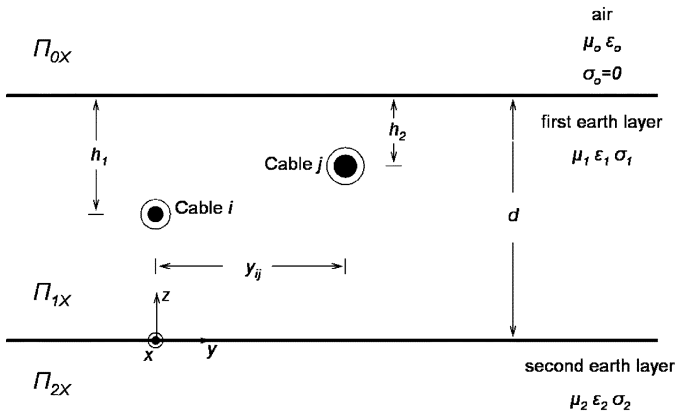

Fig. 1. Geometric configuration of two SC underground cables in a two-layer earth.

II. Problem Formulation and Solution

A. EM-Field Equations

In Fig. 1, two SC cables i, j are buried in the first layer of a two-layer earth. The second layer is considered to be of infinite depth. The first layer has permeability μ_1, permittivity ε_1, and conductivity σ_1, while the corresponding properties of the

Manuscript received September 1, 2004; revised October 21, 2004. Paper no. TPWRD-00403-2004.

The authors are with the Power Systems Laboratory, Department of Electrical and Computer Engineering, Aristotle University of Thessaloniki, Thessaloniki GR-54124, Greece (e-mail: grigoris@eng.auth.gr).

Digital Object Identifier 10.1109/TPWRD.2005.848737

second earth layer are $\mu_2, \varepsilon_2, \sigma_2$. The air has a conductivity σ_0 equal to zero and permeability μ_0 and permittivity ε_0 equal to those of the free space.

The mutual impedances between conductors may be derived by integrating the field due to the conductor dipoles. The field intensities and potentials can be expressed in terms of a single vector function Π, usually referred to as the Hertzian vector [3].

The Π function has been adopted for the solution of the EM field in this paper.

Assuming a horizontal dipole in the place of cable i in Fig. 1, the x components of the Π function in the air, in the first and in the second earth layer are defined as $\Pi_{\text{ox}}, \Pi_{1x}$ and Π_{2x}, respectively. The equation that describes Π_{ox} at any point in the air with coordinates (x, y, z) is [3]

$$\Pi_{\text{ox}} = \int_0^\infty f_o(u) e^{-a_o z} J_o(ru)\, du, \qquad z \geq d. \tag{1}$$

For $0 \leq z \leq d, \Pi_{1x}$ is described by the following equations:

$$\Pi_{1x} = \int_0^\infty \left[f_{1\alpha}(u) e^{-a_1 z} + g_{1a}(u) e^{a_1 z} \right] J_o(ru)\, du, \quad z \geq (d - h_1) \tag{2a}$$

and

$$\Pi_{1x} = \int_0^\infty \left[f_{1b}(u) e^{-a_1 z} + g_{1b}(u) e^{a_1 z} \right] J_o(ru)\, du, \quad z \leq (d - h_1). \tag{2b}$$

Finally, for $z \leq 0, \Pi_{2x}$ is given by

$$\Pi_{2x} = \int_0^\infty f_2(u) e^{a_2 z} J_o(ru), du, \qquad z \leq 0. \tag{3}$$

In the above relations, $J_o(\,)$ is the Bessel function of the first kind of zero order, $r = \sqrt{x^2 + y^2}, \alpha_i = \sqrt{u^2 + \gamma_i^2}, \gamma_i^2 = j\omega\mu_i(\sigma_i + j\omega\varepsilon_i)$ where $i = 0, 1, 2, j$ is the imaginary unit and $\omega = 2\pi f$ is the angular velocity.

B. Determination of the Hertzian Vector Components

Since all of the f and g functions in (1)–(3) are unknown, the determination of the Hertzian vector components is done by means of an auxiliary configuration with a known EM field solution together with the reciprocity theorem [10]. This theorem states that in a linear, bilateral, single circuit network, the ratio of excitation to response is constant, when the position of excitation and response is interchanged. The ratio of the voltage induced on cable i to the current imposed on a conductor k, located in the air or in the second earth layer, can be calculated

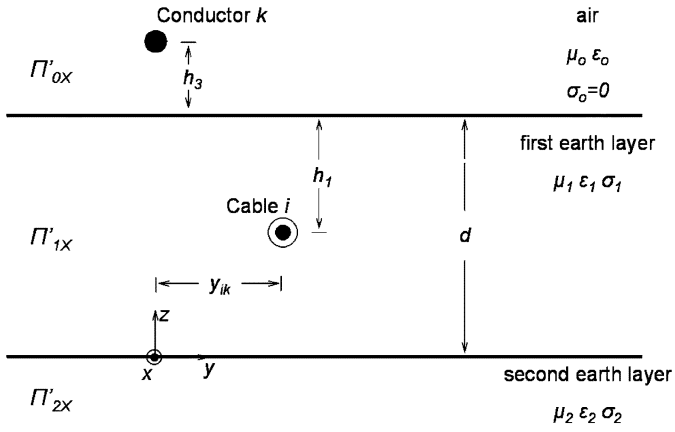

Fig. 2. Geometric configuration of an overhead conductor and an underground cable in a two-layer earth.

by existing formulas in [3]–[5]. Due to the reciprocity theorem, this ratio is equal to the corresponding voltage induced on conductor k to the current imposed on cable i.

Following the above reasoning, the auxiliary configuration of Fig. 2 is considered first. The x-components of the Π function in the different media, derived by a horizontal dipole in the place of the overhead conductor k, are given in [3]. Applying the boundary conditions at $z = d$ and $z = 0$ as given in [4], the field at any point can be fully defined. A description of the above procedure is presented in Appendix A.

The per-unit length mutual impedance between the overhead conductor k and the cable i can be derived by integrating Π'_{1x} along the infinite conductor k, that is, along the x-axis [3]

$$Z'_{ik} = \int_{-\infty}^{\infty} \left[\gamma_1^2 \frac{\Pi'_{1x(z=d-h_1, y=y_{ik})}}{IdS} \right] dx \tag{4}$$

where IdS is the moment of the dipole. By replacing Π'_{1x} with the expressions of Appendix A, Z'_{ik} takes the form of (5a)

$$Z'_{ik} = \gamma_1^2 \int_0^\infty \frac{\left[f_1(u) e^{a_1(d-h_1)} + g_1(u) e^{-a_1(d-h_1)} \right]}{IdS} \times \left[\int_{-\infty}^{\infty} J_o\left(u\sqrt{x^2 + y_{ik}^2} \right) dx \right] du. \tag{5a}$$

The term $\int_{-\infty}^{\infty} J_o(u\sqrt{x^2 + y_{ik}^2})\, dx$ can be substituted by $2\cos(uy_{ik})/u$, as in [11] and [3], resulting in (5b).

In the above procedure, the overhead conductor k was carrying the excitation current. According to the reciprocity theorem, an equation similar to (5b) can be obtained if the excitation current is imposed on the cable i, as shown in (5b) at the bottom of the page.

$$Z'_{ik} = \frac{j\omega\mu_1\mu_0}{\pi} \int_0^\infty \left\{ \frac{e^{-a_o h_3} \left[(\mu_2\alpha_1 + \mu_1\alpha_2) e^{a_1(d-h_1)} + (\mu_2\alpha_1 - \mu_1\alpha_2) e^{-a_1(d-h_1)} \right]}{\left[(\mu_0\alpha_1 + \mu_1\alpha_o)(\mu_2\alpha_1 + \mu_1\alpha_2) e^{a_1 d} + (\mu_2\alpha_1 - \mu_1\alpha_2)(\mu_1\alpha_o - \mu_0\alpha_1) e^{-a_1 d} \right]} \right\} \cos(uy_{ik})\, du. \tag{5b}$$

Thus, assuming a horizontal dipole with a moment equal to IdS in the place of cable i in Fig. 1, (1)–(3) become the equations which describe the problem. Therefore, Z'_{ik} is also given by

$$Z'_{ik} = \int_{-\infty}^{\infty} \left[\gamma_o^2 \frac{\Pi_{\text{ox}(z=d+h_3, y=-y_{ik})}}{IdS} \right] dx. \tag{6}$$

From (5b), (6), and (1), $f_o(u)$ and Π_{ox} can be derived.

A similar procedure is adopted to define Π_{2x}. Assuming a cable m buried in the second earth layer in a depth $d+h_4$ from the surface of the earth and a horizontal separation distance y_{mi} from cable i, $f_2(u)$ and Π_{2x} can be determined.

Finally, using the boundary conditions given in [4] at $z=d$ and $z=0$ in Fig. 1, the field Π_{1x} in the first earth layer is also found. The analytic expressions of the f and Π functions in (1), (2a)–(3) are shown in Appendix B.

III. Self- and Mutual-Impedance Formulas

The per-unit length mutual impedance Z'_{ij} between cables i and j is found by integrating Π_{1x} along the infinite cable i, that is, along the x-axis

$$Z'_{ij} = \int_{-\infty}^{\infty} \left[\gamma_1^2 \frac{\Pi_{1x(z=d-h_2, y=y_{ij})}}{IdS} \right] dx. \tag{7}$$

Depending on the position of cable j, Π_{1x} from (2a) or (2b) will be replaced in (7). In either case, the final form of Z'_{ij} results in (8), shown at the bottom of the page, where

$$s_{10} = (\mu_0\alpha_1 + \mu_1\alpha_o) \quad s_{21} = (\mu_2\alpha_1 + \mu_1\alpha_2)$$

and

$$d_{21} = (\mu_2\alpha_1 - \mu_1\alpha_2) \quad d_{10} = (\mu_0\alpha_1 - \mu_1\alpha_o).$$

The self-impedance of cable i results from (8), by replacing y_{ij} with the cable outermost radius r_{ii} and h_2 with h_1.

From (8), the existing formula for the calculation of underground power cables impedances for the homogeneous earth case [2], [3] can be reproduced, simply by replacing α_2 with α_1 and μ_2 with μ_1.

Replacing α_1 with α_o, μ_1 with μ_0, and setting α_o equal to u as in [3], (8) takes the form of the well-known Carson formula for the overhead line impedance above homogeneous earth.

Further observation of (8) reveals that it essentially consists of four terms.

The first and dominant one contains an exponential function which depends on the vertical distance between the cables. Both factors of this exponential function are denoted with the symbol s to indicate the sum of EM properties of the three different media involved: air, first, and second earth layer.

The second term depends on the vertical distance between one cable and the image of the other with respect to the two earth layers boundary. One factor of this term is represented with the symbol d_{21} to indicate the difference between the EM properties that determine the two earth layers. Thus, when the resistivity, permeability, and permittivity values of the two earth layers are equal, this term vanishes, as the boundary of the two layers disappears too.

The third term refers to the distance between one cable and the image of the other with respect to the air-earth boundary. One of the factors of the latter term is d_{10}, indicating the difference between the EM properties that determine the air-earth boundary. When this boundary does not exist, this term is also zero.

Finally, the fourth term contains an exponential function which depends on the distance between the image of the cable closest to the air-earth boundary with respect to that boundary and the image of the cable closest to the two earth layers limit with respect to the two earth layers boundary. As expected, this term has as factors only symbols denoted with d, because it vanishes whenever one of the two boundaries does not exist.

Equation (8) has a general form capable of handling cases with arbitrary resistivities, permittivities, and permeabilities of the earth layers. Therefore, it can be also applied in cases where the effects of a ferromagnetic region must be taken into account [4].

The proposed solution of the EM field can be generalized in order to cover various cable arrangements and multilayered earth structures. Proper analytic expressions may be derived for cases of underground conductors buried in different earth layers of multilayered earth structures as well as for combinations of underground and overhead conductors. Thus, the above procedure can be also helpful to problems of inductive interference between overhead lines and neighboring underground insulated metal pipes buried in multilayer earth or for EM compatibility problems.

IV. Numerical Integration of the Impedance Formulas

Direct numerical integration is used for the calculation of the semi-infinite integral in (8). The integral shows both regular and irregular oscillations, due to the cosine and the exponential terms respectively, as recorded also in [12] for the Pollaczek integral of [2].

It also shows an initial steep descent between zero and the first root of $\cos(uy_{ij})$.

For these reasons, the use of a single numerical integration method proved to be inefficient. To overcome these difficulties, a combination of three numerical integration methods, namely the

$$Z'_{ij} = \frac{j\omega\mu_1}{2\pi} \int_0^{\infty} \frac{\cos(uy_{ij})}{\alpha_1} \left[\frac{s_{10}s_{21}e^{-a_1|h_1-h_2|} + s_{10}d_{21}e^{-a_1(d-h_1+d-h_2)} + d_{10}s_{21}e^{-a_1(h_1+h_2)} + d_{10}d_{21}e^{-a_1(2d-|h_1-h_2|)}}{s_{10}s_{21} - d_{10}d_{21}e^{-2a_1d}} \right] du \tag{8}$$

TABLE I
TWO-LAYER EARTH MODELS

	$\rho_1(\Omega\cdot m)$	$\rho_2(\Omega\cdot m)$	d(m)
CASE I	372.729	145.259	2.690
CASE II	246.841	1058.79	2.139
CASE III	57.344	96.714	1.651
CASE IV	494.883	93.663	4.370
CASE V	160.776	34.074	1.848
CASE VI	125.526	1093.08	2.713

Gauss–Legendre method [13], the Gauss–Laguerre method [13] and the Lobatto rule [14] is used. This new integration scheme was applied successfully to the calculation of earth return impedances in cases of homogeneous earth [6] and proved to be numerically stable and very efficient. A detailed description of the methodology is presented in Appendix C.

V. FINITE-ELEMENT APPROACH

To check the accuracy of the results obtained by the new expressions, the cable impedances for the two-layer earth case are also calculated by means of a proper FEM formulation. The FEM package developed at the Power Systems Laboratory of the Aristotle University of Thessaloniki has been used. Introducing a newly developed iteratively adaptive mesh generation technique [15], this package can be applied for the computation of overhead line and underground cable parameters in unbounded discretization areas [7].

VI. NUMERICAL RESULTS

A. Comparison With the FEM

Six different two-layer earth models, based on actual grounding parameter measurements [8], are investigated. The corresponding data for the resistivities ρ_1 of the first and ρ_2 of the second layer and for the depth d of the first layer are shown in Table I. The second layer is considered to be of infinite depth.

The case of a shallowly located SC cable system is examined in the horizontal cable arrangement of Fig. 3(a) as in [16]. Cables are in a depth $h = 1.2$ m with a spacing $s = 0.25$ m. The core radius is $r_C = 23.4 * 10^{-3}$ m, while the outer radius is $r_S = 48.4 * 10^{-3}$ m. The conductivity of the cable core is $\sigma = 5.882\,35 * 10^7$ S/m, while the relative permeability $\mu_r = 1$ for all of the areas in Fig. 3.

Series impedances are calculated for this cable configuration and for the six earth models of Table I using the proposed analytic formula of (8) for the frequency range of 50 Hz–1 MHz to cover power cable operating conditions from steady-state up to very fast transients. The novel numerical integration scheme used for the calculation of the proposed formula proved to be numerically stable. The computation time for the numerical integration, using a tolerance of 10^{-8}, is less than 25 min for the derivation of 60 impedance matrices in an Intel Pentium IV PC at 2.66 GHz. When the tolerance is defined at 10^{-7}, the computational time is less than 10 min for the set of the 60 cases.

The results are compared to the corresponding obtained by the FEM. The relative differences are calculated using

$$\text{Relative difference}(\%) = \frac{\big||Z_{\text{formula}}| - |Z_{\text{FEM}}|\big|}{|Z_{\text{FEM}}|} * 100. \quad (9)$$

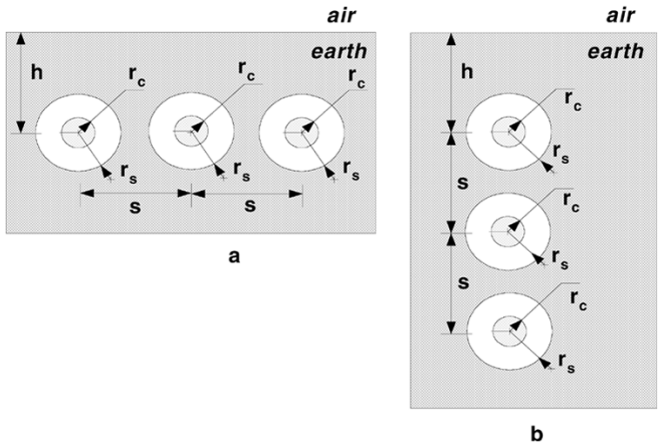

Fig. 3. (a) Horizontal and (b) vertical SC cable arrangements.

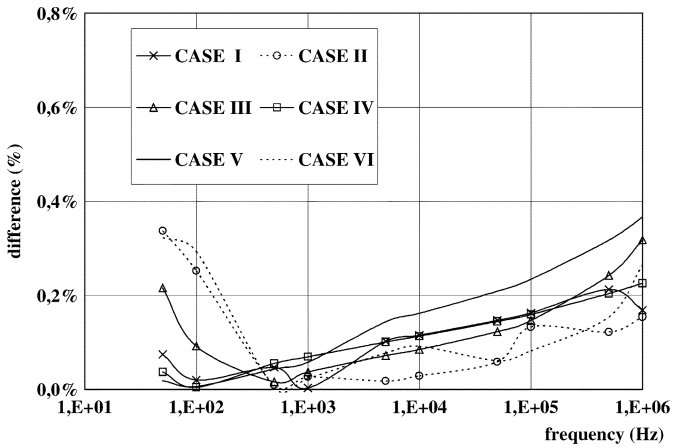

Fig. 4. Differences in the magnitude of the mutual impedance between the formula and the FEM.

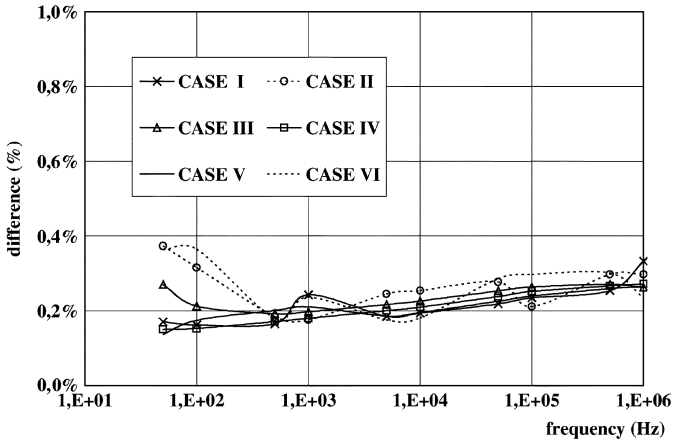

Fig. 5. Differences in the magnitude of the self-impedance between the formula and the FEM.

In Figs. 4 and 5, the relative differences for the magnitude of the mutual and self-impedances of the horizontal cable arrangement are shown, respectively. In all of the cases, the differences recorded for the impedance magnitude and phase are less than 0.9 % for the whole frequency range under consideration.

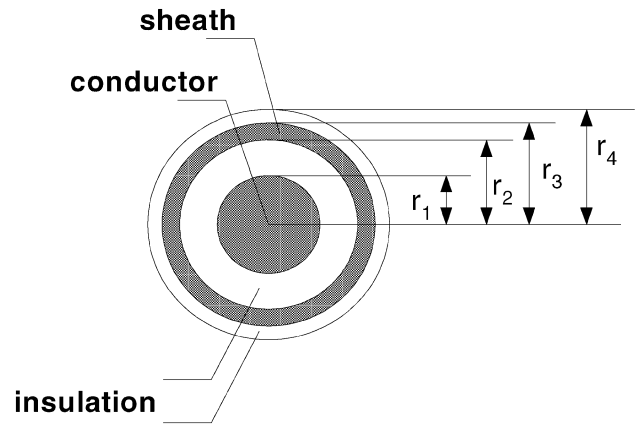

Fig. 6. SC cable with core and sheath.

TABLE II
DATA OF THE SC CABLE ARRANGEMENT OF FIG. 6

Core radius r_1	0.0234 m
Main insulation radius r_2	0.0385 m
Sheath radius r_3	0.0413 m
Outer insulation radius r_4	0.0484 m
Core resistivity	1.7 x 10^{-8} Ω·m
Resistivity of lead sheath	2.1 x 10^{-7} Ω·m
Inner insulator ε_r	3.5
Outer insulator ε_r	8.0
All relative permeability μ_r	1.0

B. Comparison With the Homogeneous Earth Results

The SC cable of Fig. 6 having a core and sheath is considered next. Original cable data from [17] are reproduced in Table II. The two cable arrangements of Fig. 3 are examined. For the vertical arrangement of Fig. 3(b), the first cable is in a depth $h = 0,75$ and $s = 0,15$ m.

The series impedances for the configurations of Fig. 3 and the six earth models of Table I are calculated for the frequency range of 50 Hz to 10 MHz using the new analytic formulas. The results are now compared to the impedances obtained by the CABLE CONSTANTS/PARAMETERS supporting routine of the EMTP for homogeneous earth with resistivity equal to the resistivity of the first earth layer.

The differences, calculated by (10), are shown in Figs. 7 and 8 for the magnitude of the mutual and self cable impedances

$$\text{Relative difference } (\%) = \frac{(|Z_{\text{two-layer}}| - |Z_{\text{homogeneous}}|)}{|Z_{\text{homogeneous}}|} * 100. \tag{10}$$

In the above diagrams, it is shown that differences from 10% up to 40% are encountered. The differences are greater for the mutual impedances, as the EM-field path is through the ground. The differences are also maximized when the resistivities of the two layers show a significant divergence. Also in the high-frequency range, over 100 kHz, the differences become greater due to the approximations used in earth return impedance calculation in the EMTP CABLE CONSTANTS supporting routine [6].

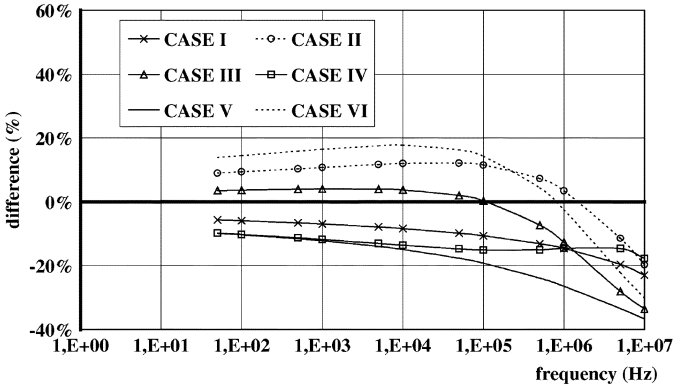

Fig. 7. Differences in the magnitude of the mutual impedance of the cables sheaths between the two-layer and the homogeneous earth models. Horizontal cable arrangement.

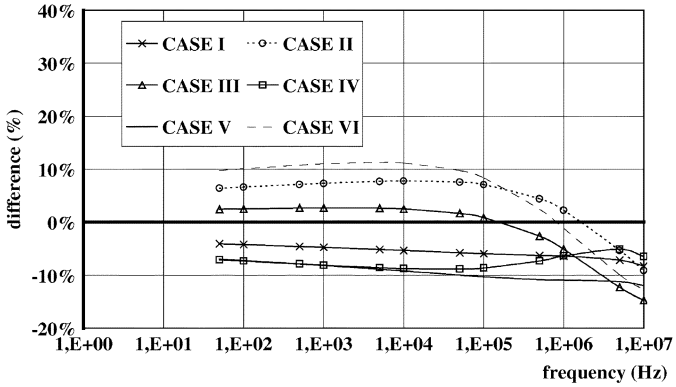

Fig. 8. Differences in the magnitude of the self-impedances between the two-layer and the homogeneous earth models. Vertical cable arrangement.

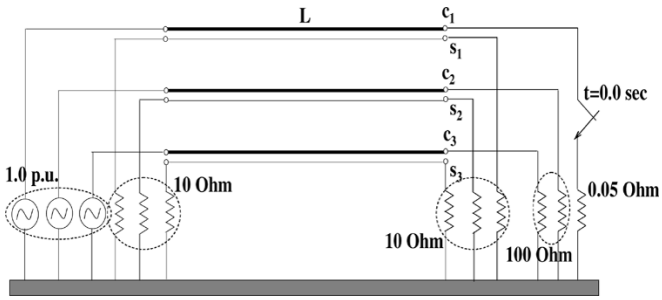

Fig. 9. System diagram of the single line-to-ground short-circuit test.

C. Influence of Earth Stratification on Cable Transient Response

In order to show the influence of the earth stratification on the actual transient voltages and currents, a simple transient in a cable configuration is examined. The test configuration adopted from [17] is shown in Fig. 9. The SC cable of Fig. 6 is used in the horizontal arrangement of Fig. 3(a), with a length L varying from 1 to 10 km. A three-phase balanced sinusoidal voltage source with a peak magnitude of 1.0 p.u. is connected at the sending end of the cable. The cable sheaths are grounded at both sending and receiving ends with 10-Ω resistances. A balanced ohmic load of 100 Ω is connected at the receiving end. A single line-to-ground fault is applied at the receiving end of core 1 through a resistance of 0.05 Ω at time zero.

First, the cable configuration of Fig. 9 is considered to be buried in a two-layer earth having the characteristics of the six

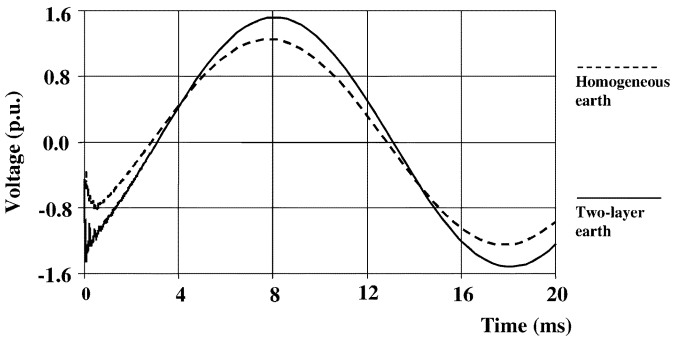

Fig. 10. Cable 2 receiving-end voltage. Two-layer earth CASE IV versus homogeneous earth model for the 5-km-long three SC cable arrangement.

cases of Table I. A time-domain transmission-line model is used with distributed parameters calculated using the results obtained by the new formulas. Next, in the same cable model, the earth is assumed to be homogeneous with a resistivity equal to the resistivity of the first layer. The transient voltages and currents are calculated using the EMTP.

In Fig. 10, the voltage at the receiving end of core 2 for CASE IV of the two-layer earth cases defined in Table I, for a cable length of 5 km, is superimposed on the corresponding curve for the homogeneous earth.

Results show that the differences in the cable impedances between the homogeneous and the two-layer earth models affect also significantly the transient response of the system. The voltages and currents for the stratified earth were 9% up to 30% higher than the corresponding for the homogenous earth in all examined cases. The divergences depend also upon the cable length, as the length influences the frequency of the traveling waves and, therefore, also the differences in the cable impedances, according to Figs. 7 and 8.

VII. Conclusion

The problem of the calculation of the earth return impedances of underground SC power cables buried in a two-layer earth is addressed in this paper. A rigorous solution of the EM field is presented, leading to new analytic expressions for the self and mutual impedance. The new formulas can be generalized to cover other cable arrangements and multilayer earth models.

For the numerical evaluation of the semi-infinite integrals involved in the derived expressions, a novel numerical integration scheme, based on proper combinations of three integration methods, is used. The proposed formulation is applied for the case of typical SC power cable systems, buried in the first layer of a variable two-layer earth structure. To check the accuracy of the results obtained by the new expressions, they are compared to those obtained by an FEM formulation. The recorded differences in the self and mutual impedance magnitudes and arguments are less than 0.9% over a wide frequency range, covering almost all possible power cable operational cases. The integration scheme proved to be numerically stable and efficient in all examined cases.

The results obtained by the new expressions show significant differences from the corresponding results for the homogeneous earth case, where the resistivity of the earth is considered to be equal to the resistivity of the first layer. These differences are amplified in the high-frequency region, due to the approximations incorporated in the numerical calculation of the earth correction factors in the CABLE CONSTANTS/PARAMETERS supporting routine of the EMTP.

Finally, a switching transient simulation is examined using the impedances calculated for the two-layer earth cases. Earth stratification seems to influence transient responses significantly, leading to higher transient voltages and currents. Therefore, it cannot be ignored.

The proposed analytic expressions together with the new numerical integration scheme constitute a useful tool in the development of transient underground cable models. They eliminate the need for assumptions in the numerical evaluation of the earth correction terms and enhance the simulation of various earth structures. They may be also adopted in most of the commonly used transmission line or power cable parameter calculation software packages.

Appendix

A. Field Derived by the Overhead Conductor Dipole

In Fig. 2, the equations that describe the EM field at any point with coordinates (x, y, z) are [3], [4]

$$\Pi'_{\text{ox}} = \int_0^\infty \left[C\frac{u}{a_o} e^{-a_o|z-(d+h_3)|} + g_o(u)e^{-a_o z} \right] J_o(ru)\,du, \quad z \geq d \tag{A.1}$$

$$\Pi'_{1x} = \int_0^\infty \left[f_1(u)e^{a_1 z} + g_1(u)e^{-a_1 z} \right] J_o(ru)\,du, \quad 0 \leq z \leq d \tag{A.2}$$

$$\Pi'_{2x} = \int_0^\infty f'_2(u)e^{a_2 z} J_o(ru)\,du, \qquad z \leq 0 \tag{A.3}$$

where $C = (j\omega\mu_0 IdS)/(4\pi\gamma_o^2)$.

The boundary conditions at $z = d$ are [4]

$$\gamma_o^2 \Pi'_{\text{ox}} = \gamma_1^2 \Pi'_{1x}, \tag{A.4}$$

$$\frac{1}{\mu_0}\gamma_o^2 \frac{\partial \Pi'_{\text{ox}}}{\partial z} = \frac{1}{\mu_1}\gamma_1^2 \frac{\partial \Pi'_{1x}}{\partial z} \tag{A.5}$$

whereas the corresponding boundary conditions at $z = 0$ are [4]

$$\gamma_1^2 \Pi'_{1x} = \gamma_2^2 \Pi'_{2x}, \tag{A.6}$$

$$\frac{1}{\mu_1}\gamma_1^2 \frac{\partial \Pi'_{1x}}{\partial z} = \frac{1}{\mu_2}\gamma_2^2 \frac{\partial \Pi'_{2x}}{\partial z}. \tag{A.7}$$

Substituting (A.1)–(A.3) in (A.4)–(A7), the following equations are derived:

$$\gamma_o^2 \left(C\frac{u}{a_o} e^{-a_o h_3} + g_o e^{-a_o d} \right) = \gamma_1^2 \left(f_1 e^{a_1 d} + g_1 e^{-a_1 d} \right) \tag{A.8}$$

$$\frac{a_o}{\mu_0}\gamma_o^2 \left(C\frac{u}{a_o} e^{-a_o h_3} - g_o e^{-a_o d} \right) = \frac{\alpha_1}{\mu_1}\gamma_1^2 \left(f_1 e^{a_1 d} - g_1 e^{-a_1 d} \right) \tag{A.9}$$

$$\gamma_1^2 (f_1 + g_1) = \gamma_2^2 f'_2 \tag{A.10}$$

$$\frac{a_1}{\mu_1}\gamma_1^2(f_1-g_1)=\frac{\alpha_2}{\mu_2}\gamma_2^2 f_2'. \tag{A.11}$$

Solving the system of (A.8)–(A.11), f_1 and g_1 are obtained and shown in (A.12) and (A.13), respectively, shown at the bottom of the page. Thus, the Π function in the first layer Π_{1x}' is completely defined.

B. Field Derived by the Underground Cable Dipole

Combining (1) and (6), the per-unit length mutual impedance Z_{ik}' between the cable i and the overhead conductor k is also given by

$$Z_{ik}'=\gamma_o^2\int_0^\infty \frac{2f_o(u)e^{-a_o(d+h_3)}}{IdS}\frac{\cos(uy_{ik})}{u}\,du \tag{A.14}$$

From (A.14) and (5b), the resulting expression for $f_o\ (u)$ is derived and shown in (A.15), at the bottom of the page, where $C_1=(j\omega\mu_1 IdS)/(4\pi\gamma_1^2)$. Thus, $\Pi_{\rm ox}$ in (1) is fully determined.

The function $f_2\ (u)$ can be found using a similar procedure. The per-unit length mutual impedance between cables i and m can be produced by (5b), after the replacement of the variables corresponding to the air with those of the second earth layer. Its analytic form is shown in (A.16), shown in the equation at the bottom of the page. Due to the reciprocity theorem, the same impedance is given by an equation similar to (A.14), but for the second earth layer

$$Z_{mi}'=\gamma_2^2\int_0^\infty \frac{2f_2(u)e^{-a_2h_4}}{IdS}\frac{\cos(uy_{mi})}{u}\,du \tag{A.17}$$

From (A.16) and (A.17), $f_2(u)$ is derived and its analytic form is shown in (A.18), at the bottom of the page. Thus, Π_{2x} in (3) is also determined.

Applying the boundary conditions (A.4)–(A.7) [4] for the system of (1), (2a)–(3), the following are derived:

$$\gamma_o^2\left(2C_1u\frac{\gamma_1^2}{\gamma_o^2}\mu_0\mathrm{K}_1(u)\right)=\gamma_1^2\left(f_{1a}(u)e^{-a_1d}+g_{1a}(u)e^{a_1d}\right) \tag{A.19}$$

$$-\frac{a_o}{\mu_0}\gamma_o^2\left(2C_1u\frac{\gamma_1^2}{\gamma_o^2}\mu_0\mathrm{K}_1(u)\right)=\frac{\alpha_1}{\mu_1}\gamma_1^2\left(-f_{1a}(u)e^{-a_1d}+g_{1a}(u)e^{a_1d}\right) \tag{A.20}$$

$$\gamma_1^2(f_{1b}(u)+g_{1b}(u))=\gamma_2^2\left(2C_1u\frac{\gamma_1^2}{\gamma_2^2}\mu_2\mathrm{K}_2(u)\right) \tag{A.21}$$

$$\frac{a_1}{\mu_1}\gamma_1^2(-f_{1b}(u)+g_{1b}(u))=\frac{\alpha_2}{\mu_2}\gamma_2^2\left(2C_1u\frac{\gamma_1^2}{\gamma_2^2}\mu_2\mathrm{K}_2(u)\right). \tag{A.22}$$

From (A.19)–(A.22), $f_{1a}(u), \mathrm{g}_{1a}(u), f_{1b}(u)$, and $g_{1b}(u)$ are derived. Thus, Π_{1x} in (2), can be defined and is shown in (A.23)

$$\Pi_{1x}=\int_0^\infty\left[\frac{C_1u}{a_1}(\mu_0\alpha_1+\mu_1\alpha_o)\mathrm{K}_1(u)e^{a_1(d-z)}+\frac{C_1u}{a_1}(\mu_0\alpha_1-\mu_1\alpha_o)\mathrm{K}_1(u)e^{-a_1(d-z)}\right]J_o(ru)\,du,\qquad z\geq(d-h_1) \tag{A.23a}$$

$$\Pi_{1x}=\int_0^\infty\left[\frac{C_1u}{a_1}(\mu_2\alpha_1-\mu_1\alpha_2)\mathrm{K}_2(u)e^{-a_1z}+\frac{C_1u}{a_1}(\mu_2\alpha_1+\mu_1\alpha_2)\mathrm{K}_2(u)e^{a_1z}\right]J_o(ru)\,du,\qquad z\leq(d-h_1) \tag{A.23b}$$

$$f_1(u)=\frac{2\gamma_o^2\mu_1 Cue^{-a_oh_3}(\mu_2\alpha_1+\mu_1\alpha_2)}{\gamma_1^2\left[(\mu_0\alpha_1+\mu_1\alpha_o)(\mu_1\alpha_2+\mu_2\alpha_1)e^{a_1d}+(\mu_1\alpha_o-\mu_0\alpha_1)(\mu_2\alpha_1-\mu_1\alpha_2)e^{-a_1d}\right]} \tag{A.12}$$

$$g_1(u)=\frac{2\gamma_o^2\mu_1 Cue^{-a_oh_3}(\mu_2\alpha_1-\mu_1\alpha_2)}{\gamma_1^2\left[(\mu_0\alpha_1+\mu_1\alpha_o)(\mu_1\alpha_2+\mu_2\alpha_1)e^{a_1d}+(\mu_1\alpha_o-\mu_0\alpha_1)(\mu_2\alpha_1-\mu_1\alpha_2)e^{-a_1d}\right]} \tag{A.13}$$

$$f_o(u)=2C_1u\frac{\gamma_1^2}{\gamma_o^2}\mu_0\left\{\frac{e^{a_od}\left[(\mu_2\alpha_1+\mu_1\alpha_2)e^{a_1(d-h_1)}+(\mu_2\alpha_1-\mu_1\alpha_2)e^{-a_1(d-h_1)}\right]}{\left[(\mu_0\alpha_1+\mu_1\alpha_o)(\mu_2\alpha_1+\mu_1\alpha_2)e^{a_1d}+(\mu_2\alpha_1-\mu_1\alpha_2)(\mu_1\alpha_o-\mu_0\alpha_1)e^{-a_1d}\right]}\right\}=2C_1u\frac{\gamma_1^2}{\gamma_o^2}\mu_0K_1(u)e^{a_od} \tag{A.15}$$

$$Z_{mi}'=\frac{j\omega\mu_1\mu_2}{\pi}\int_0^\infty\left\{\frac{e^{-a_2h_4}\left[(\mu_0\alpha_1+\mu_1\alpha_0)e^{a_1h_1}+(\mu_0\alpha_1-\mu_1\alpha_0)e^{-a_1h_1}\right]}{\left[(\mu_0\alpha_1+\mu_1\alpha_o)(\mu_2\alpha_1+\mu_1\alpha_2)e^{a_1d}+(\mu_0\alpha_1-\mu_1\alpha_0)(\mu_1\alpha_2-\mu_2\alpha_1)e^{-a_1d}\right]}\right\}\cos(uy_{mi})\,du \tag{A.16}$$

$$f_2(u)=2C_1u\frac{\gamma_1^2}{\gamma_2^2}\mu_2\left\{\frac{\left[(\mu_0\alpha_1+\mu_1\alpha_o)e^{a_1h_1}+(\mu_0\alpha_1-\mu_1\alpha_o)e^{-a_1h_1}\right]}{\left[(\mu_0\alpha_1+\mu_1\alpha_o)(\mu_2\alpha_1+\mu_1\alpha_2)e^{a_1d}+(\mu_2\alpha_1-\mu_1\alpha_2)(\mu_1\alpha_o-\mu_0\alpha_1)e^{-a_1d}\right]}\right\}=2C_1u\frac{\gamma_1^2}{\gamma_2^2}\mu_2K_2(u) \tag{A.18}$$

C. Numerical Integration Method

For the calculation of (8), three numerical integration methods are implemented as follows:

When the term $\cos(uy_{ij})$ is not equal to one, the interval between zero and the first root of $\cos(uy_{ij})$ is divided into the following subintervals $(0, (\pi \cdot 10^{-6})/(2y_{ij})), ((\pi \cdot 10^{-6})/(2y_{ij}), (\pi \cdot 10^{-5})/(2y_{ij})), ((\pi \cdot 10^{-5})/(2y_{ij}), (\pi \cdot 10^{-4})/(2y_{ij})) \ldots, ((0.1 \cdot \pi)/(2y_{ij}), (\pi/2y_{ij}))$. In each of these subintervals, the complex integral of (8) is calculated using the shifted 16-point Gauss–Legendre method [13]. Then, in the intervals between the subsequent roots of $\cos(uy_{ij})$, the 18-point Lobatto rule [14] is used. The procedure stops when the absolute value of the calculated integral between two subsequent roots is less than a user-predefined tolerance for both the real and the imaginary part of the integral.

If the horizontal distance y_{ij} is zero, the integration procedure is different. The shifted 16-point Gauss–Legendre method is again applied in the same way between zero and $u_o = 2\pi$. Then, the shifted 35-point Gauss–Laguerre method [13] is used for the evaluation of the rest of the integral, after the integrand is scaled by the term $e^{|h_1 - h_2|u}$. The procedure is repeated iteratively. In each iteration, the use of the Gauss–Legendre method is extended by $2u_o$ intervals to the right of u_o, while the Gauss–Laguerre method is implemented for the calculation of the rest integral until infinity. Convergence is achieved when the absolute difference between two succedent values of the calculated integral is less than a user-predefined tolerance.

REFERENCES

[1] J. R. Carson, "Wave propagation in overhead wires with ground return," *Bell Syst. Tech. J.*, no. 5, pp. 539–554, 1926.

[2] F. Pollaczek, "Ueber das feld einer unendlich langen wechselstrom-durchflossenen einfachleitung," *Elektrische Nachrichtentechnik*, vol. 3, no. 4, pp. 339–359, 1926.

[3] E. D. Sunde, *Earth Conduction Effects in Transmission Systems*, 2nd ed. New York: Dover, 1968, pp. 30–33. 99–139.

[4] M. Nakagawa, A. Ametani, and K. Iwamoto, "Further studies on wave propagation in overhead transmission lines with earth return: Impedance of stratified earth," *Proc. Inst. Elect. Eng.*, vol. 120, no. 12, pp. 1521–1528, 1973.

[5] M. Nakagawa and K. Iwamoto, "Earth return impedance for the multi-layer case," *IEEE Trans. Power App. Syst.*, vol. PAS-95, no. 2, pp. 671–676, Mar./Apr. 1976.

[6] G. K. Papagiannis, D. A. Tsiamitros, G. T. Andreou, D. P. Labridis, and P. S. Dokopoulos, "Earth return impedances of underground cables for the multi-layer case-A finite element approach," in *Proc. IEEE Power Tech Conf.*, vol. 3, 2003, pp. 1005–1011.

[7] G. K. Papagiannis, D. G. Triantafyllidis, and D. P. Labridis, "A one-step finite element formulation for the modeling of single and double circuit transmission lines," *IEEE Trans. Power Syst.*, vol. 15, no. 1, pp. 33–38, Feb. 2000.

[8] J. L. del Alamo, "A comparison among different techniques to achieve an optimum estimation of electrical grounding parameters in two-layered earth," *IEEE Trans. Power Del.*, vol. 8, no. 4, pp. 1890–1899, Oct. 1993.

[9] H. W. Dommel, *Electromagnetic Transients Program Reference Manual*. Portland, OR: Bonneville Power Administration, 1986, pp. 5-15–5-22.

[10] *The Electrical Engineering Handbook*, CRC, Boca Raton, FL, 1993, pp. 77–79.

[11] *Handbook of Mathematical Functions*, Dover, New York, 1972, pp. 479–494.

[12] F. A. Uribe, J. L. Naredo, P. Moreno, and L. Guardado, "Algorithmic evaluation of underground cable earth impedances," *IEEE Trans. Power Del.*, vol. PWRD-19, no. 1, pp. 316–322, Jan. 2004.

[13] A. Ralston and P. Rabinowitch, *A First Course in Numerical Analysis*, 2nd ed. New York: McGraw-Hill, 1988, pp. 100–106.

[14] P. Davies and P. Rabinowitch, *Methods of Numerical Integration*, 2nd ed. New York: Academic, 1984, pp. 104–223.

[15] D. P. Labridis, "Comparative presentation of criteria used for adaptive finite element mesh generation in multiconductor eddy current problems," *IEEE Trans. Magn.*, vol. 36, no. 1, pp. 267–280, Jan. 2000.

[16] Y. Yin and H. W. Dommel, "Calculation of frequency dependent impedances of underground power cables with finite element method," *IEEE Trans. Magn.*, vol. 25, no. 4, pp. 3025–3027, Jul. 1989.

[17] T.-C. Yu and J. R. Marti, "A robust phase-coordinates frequency-dependent underground cable model (zCable) for the EMTP," *IEEE Trans. Power Del.*, vol. 18, no. 1, pp. 189–194, Feb. 2003.

Dimitrios A. Tsiamitros was born in Kozani, Greece, on March 19, 1979. He received the Dipl.-Eng. degree from the Department of Electrical and Computer Engineering, Aristotle University of Thessaloniki, Thessaloniki, Greece, in 2001.

Since 2001, he has been a Postgraduate student at the Department of Electrical and Computer Engineering, Aristotle University of Thessaloniki. His interests are power system modeling and computation of electromagnetic transients.

Grigoris K. Papagiannis (S'79–M'88) was born in Thessaloniki, Greece, on September 23, 1956. He received the Dipl.-Eng. and Ph.D. degrees from the Department of Electrical Engineering from Aristotle University of Thessaloniki, Thessaloniki, Greece, in 1979 and 1998, respectively.

Since 1981 he has been a Research Assistant and since 1998, a Lecturer at the Power Systems Laboratory, Department of Electrical and Computer Engineering, Aristotle University of Thessaloniki. His special interests are power systems modeling, computation of electromagnetic transients, and power-line communications.

Dimitris P. Labridis (S'88–M'90–SM'00) was born in Thessaloniki, Greece, on July 26, 1958. He received the Dipl.-Eng. and Ph.D. degrees from the Department of Electrical Engineering at the Aristotle University of Thessaloniki, Thessaloniki, Greece, in 1981 and 1989, respectively.

Currently, he is Associate Professor in the Department of Electrical Engineering, Aristotle University of Thessaloniki. From 1982 to 2001, he was a Research Assistant and then a Lecturer and Assistant Professor in the Department of Electrical Engineering, Aristotle University of Thessaloniki. His interests include power system analysis with a special emphasis on the simulation of transmission and distribution systems, electromagnetic and thermal field analysis, numerical methods in engineering, and artificial intelligence applications in power systems and power-line communications.

Petros S. Dokopoulos (M'77) was born in Athens, Greece, in September 1939. He received the Dipl. Eng. degree from the Technical University of Athens, Athens, Greece, in 1962 and the Ph.D. degree from the University of Brunswick, Brunswick, Germany, in 1967.

From 1962 to 1967, he was with the Laboratory for High Voltage and Transmission at the University of Brunswick; from 1967 to 1974, he was with the Nuclear Research Center, Julich, Germany; and from 1974 to 1978, he was with the Joint European Torus, Oxfordshire, U.K. Since 1978, he has been Full Professor at the Department of Electrical Engineering, Aristotle University of Thessaloniki, Thessaloniki, Greece. He has many publications and seven patents on these subjects. He has been a Consultant to Brown Boveri and Cie, Mannheim, Germany; Siemens, Erlangen, Germany; Public Power Corporation, Athens, Greece; and the National Telecommunication Organization, Athens, and construction companies in Greece. His fields of interest are dielectrics, power switches, power generation (conventional and fusion), transmission, distribution, and control in power systems.